arXiv:1206.6621v2 [quant-ph] 2 Jul 2012

Nonlinear coupling between excited atoms and surface polaritons

Sofia Ribeiro[1], Stefan Y. Buhmann[1] and Stefan Scheel[1,2]
[1] *Quantum Optics and Laser Science, Blackett Laboratory, Imperial College London,*
Prince Consort Road, London SW7 2BW, United Kingdom and
[2] *Institut für Physik, Universität Rostock, Universitätsplatz 3, D-18051 Rostock, Germany*

(Dated: July 3, 2012)

Casimir–Polder interactions between an atom and a macroscopic body are typically regarded as due to the exchange of virtual photons. This is strictly true only at zero temperature. At finite temperature, real-photon exchange can provide a significant contribution to the overall dispersion interaction. Here we describe a new two-photon resonant process between an atom and a planar interface. In order to understand recent experimental results with hot atomic vapours in glass microcells, we derive a quantum mechanical description in order to understand in detail the possible coupling between atoms and surface polaritons. We derive a nonlinear effective Hamiltonian to explain how atoms can couple resonantly to the surface polariton modes of the dielectric medium which leads to second-order energy exchanges.

PACS numbers: 12.20.-m, 42.50.Nn, 71.36.+c

I. INTRODUCTION

Fluctuation-induced forces such as Casimir–Polder (CP) forces between atoms or molecules and macroscopic bodies are manifestations of the zero-point energy of the electromagnetic vacuum [1]. They occur even if the atom and the macroscopic body are in their respective (unpolarized) ground states [2] and can be understood — at least in the nonretarded limit — as interactions between a spontaneously generated atomic dipole and its (instantaneous) image inside the macroscopic body. As soon as it became possible to achieve atom-surface distances below 100μm, experiments revealed that the coupling between the atom and the surface at these short distances would produce significant effects [3].

Following the advances in laser cooling and trapping techniques in the 1980s, a new area of research has emerged. Modern laser-based techniques have allowed an unprecedented amount of control, with this control came the ability to study very large atom-based systems. As a result of these advances, trapping and manipulating single atoms, driving atoms into highly excited Rydberg states or creating Bose-Einstein condensates have become possible. New complex microstructures like atom chips allow one to trap, cool and manipulate ensembles of ultracold atoms in the vicinity of a surface [4].

Atoms and surface polaritons are very distinct quantum objects with different characteristics which make them suitable to perform different tasks. Atoms are very good candidates for storing and manipulating quantum information. The extremely promising results in the field of Rydberg atoms, both in ultracold atoms or in thermal vapours, shown that they make very good candidates to built quantum gates [5, 6]. The renewed experimental interest in Rydberg atoms is due to the unique opportunities afforded by their exaggerated properties [7] which make them extremely sensitive to small-scale perturbations of their environment and to dispersion forces. Previous work [8] showed that these properties includes massive level shifts that a Rydberg atom experiences in close proximity of another atom or in the vicinity of a macroscopic body, with shifts on the order of several GHz expected at micrometer distances.

Surface polaritons appear at the interface of two media. They represent particular solutions of the Maxwell equations which correspond to waves propagating in parallel to the interface and whose amplitude decreases exponentially when moving away from the surface. They are capable of interacting and be moved around on a surface, making them very attractive means of transporting quantum information from one point to another [9]. Upon taking advantage of the individual properties of atoms and surface polaritons and their different properties, it is possible to propose sophisticated quantum circuits [10].

Atom-polariton couplings lead to the (nonresonant) CP interaction between an atom and a planar interface. In the nonretarded limit, this interaction scales with $1/z^3$ (z is the atom-surface distance) [2]. Moreover, it has already been shown that it is possible to turn the (usually attractive) CP interaction into a repulsive force by a resonant coupling between a virtual emission of an atom and a virtual excitation of a surface polariton [11]. Similarly, it has been shown that the atom-surface coupling can drastically modify atomic branching ratios, because of surface-induced enhancement of a resonant decay channel [12].

In this article we analyze a new type of near-field effect involving surface polaritons inspired by the experiment of Kübler *et al.* [13] with hot Rb vapour in glass cells. Their experiment indicated that a description of the atom-surface interactions should also include a nonlinear coupling between the atomic transitions and surface polaritons. Their experimental results indicated that it should be possible for an atom to be coupled resonantly to the surface polariton modes of the dielectric material which leads to second-order energy exchanges with the atomic transition energy matching the difference in polariton energies.

The article is organised as follows. After briefly reviewing the formalism of macroscopic QED in Sec. II, we derive an effective nonlinear atom-polariton coupling Hamiltonian is Sec. III and give concluding remarks in Sec. IV.

II. BASIC EQUATIONS

In the electric dipole approximation, the Hamiltonian that governs the dynamics of the coupled atom-field system can be written as [2]

$$\hat{H} = \int_0^\infty d\omega \int d^3r\, \hbar\omega\, \hat{\mathbf{f}}^\dagger(\mathbf{r},\omega)\cdot\hat{\mathbf{f}}(\mathbf{r},\omega) + \sum_n \hbar\omega_n \hat{A}_{nn} - \sum_{m,n} \hat{A}_{mn}\mathbf{d}_{mn}\cdot\hat{\mathbf{E}}(\mathbf{r}_A)\,. \tag{1}$$

It is expressed in terms of a set of bosonic variables $\hat{\mathbf{f}}^\dagger(\mathbf{r},\omega)$ and $\hat{\mathbf{f}}(\mathbf{r},\omega)$ that have the interpretation as amplitude operators for the elementary excitations of the system composed of the electromagnetic field and absorbing medium. They obey the commutation rules

$$[\hat{f}_k(\mathbf{r},\omega), \hat{f}^\dagger_{k'}(\mathbf{r}',\omega')] = \delta_{kk'}\delta(\omega-\omega')\delta(\mathbf{r}-\mathbf{r}')\,. \tag{2}$$

The relevant part of the Hamiltonian for our study is the interaction Hamiltonian

$$\hat{H}_{\text{int}} = -\sum_{n,m}\hat{A}_{nm}\mathbf{d}_{nm}\cdot\hat{\mathbf{E}}(\mathbf{r}_A), \tag{3}$$

in which the $\hat{A}_{nm}$ denote the transition operators between two dipole-coupled internal atomic states $|m\rangle$ and $|n\rangle$ with dipole transition matrix elements $\mathbf{d}_{nm} = \langle n|\,\hat{\mathbf{d}}\,|m\rangle$. The frequency components of the electric field operator

$$\hat{\mathbf{E}}(\mathbf{r}_A) = \int_0^\infty d\omega\, \hat{\mathbf{E}}(\mathbf{r}_A,\omega) + \text{h.c.} \tag{4}$$

are constructed via a source-quantity representation from the dynamical variables $\hat{\mathbf{f}}^\dagger(\mathbf{r},\omega)$ and $\hat{\mathbf{f}}(\mathbf{r},\omega)$ as

$$\hat{\mathbf{E}}(\mathbf{r}_A,\omega) = \int d^3r\, \boldsymbol{G}_e(\mathbf{r}_A,\mathbf{r},\omega)\cdot\hat{\mathbf{f}}(\mathbf{r},\omega)\,. \tag{5}$$

The tensor $\boldsymbol{G}_e(\mathbf{r}_A,\mathbf{r},\omega)$ is related to the classical Green tensor $\boldsymbol{G}(\mathbf{r}_A,\mathbf{r},\omega)$ by

$$\boldsymbol{G}_e(\mathbf{r},\mathbf{r}',\omega) = i\frac{\omega^2}{c^2}\sqrt{\frac{\hbar}{\varepsilon_0\pi}\operatorname{Im}\varepsilon(\mathbf{r}',\omega)}\,\boldsymbol{G}(\mathbf{r},\mathbf{r}',\omega). \tag{6}$$

The Green tensor itself is a solution of the Helmholtz equation

$$\left[\boldsymbol{\nabla}\times\boldsymbol{\nabla}\times-\frac{\omega^2}{c^2}\varepsilon(\mathbf{r},\omega)\right]\boldsymbol{G}(\mathbf{r},\mathbf{r}',\omega) = \delta(\mathbf{r}-\mathbf{r}') \tag{7}$$

together with the boundary condition $\boldsymbol{G}(\mathbf{r},\mathbf{r}',\omega)\to\mathbf{0}$ for $|\mathbf{r}-\mathbf{r}'|\to\infty$. The Green tensor obeys the useful integral relation

$$\int d^3s\,\frac{\omega^2}{c^2}\operatorname{Im}\varepsilon(\mathbf{s},\omega)\,\boldsymbol{G}(\mathbf{r},\mathbf{s},\omega)\cdot\boldsymbol{G}^*(\mathbf{s},\mathbf{r}',\omega) = \operatorname{Im}\boldsymbol{G}(\mathbf{r},\mathbf{r}',\omega)\,, \tag{8}$$

which follows directly from the Helmholtz equation (7) and which reflects the linear fluctuation-dissipation theorem.

III. EFFECTIVE ATOM-POLARITON COUPLING

In this section, we derive the quantum mechanical description for an effective nonlinear atom-polariton interaction. The situation we envisage is depicted in Fig. 1 in which an atomic transition couples resonantly to two surface polariton modes of the dielectric material. This corresponds to second order energy exchanges with the atomic transition energy matching the difference in polariton energies. To illustrate our basic idea, we consider the interaction of an atomic transition of frequency ω_{10} between two eigenstates $|0\rangle$ and $|1\rangle$ with two surface polaritons with corresponding center frequencies Ω_1 and Ω_2 ($\Omega_1 \neq \Omega_2$) for whom the condition $\Omega_1 \approx \omega_{10} + \Omega_2$ is satisfied. The polariton resonance frequencies Ω_1 and Ω_2 are assumed to be far from any other atomic transition frequency ω_{mn}.

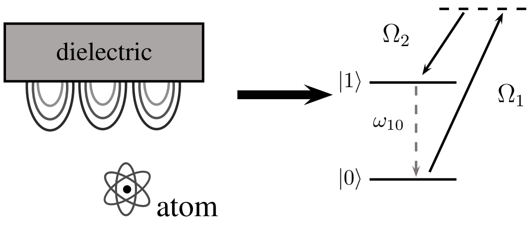

FIG. 1: Scheme of resonance between the atomic transition and one surface polariton which leads to the creation of a second polariton $\Omega_1 \approx \omega_{10} + \Omega_2$.

Heisenberg's equations of motion for the dynamical variables and the atomic transition operators follow from the Hamiltonian (1) as

$$\dot{\hat{\mathbf{f}}}(\mathbf{r},\omega,t) = -i\omega\hat{\mathbf{f}}(\mathbf{r},\omega) + \frac{1}{\sqrt{\hbar\pi\varepsilon_0}}\frac{\omega^2}{c^2}\sqrt{\operatorname{Im}\varepsilon(\mathbf{r},\omega)}\sum_{k,l}\hat{A}_{kl}\mathbf{d}_{kl}\cdot\boldsymbol{G}^*(\mathbf{r}_A,\mathbf{r},\omega)\,, \tag{9}$$

$$\dot{\hat{A}}_{mn}(t) = i\omega_{mn}\hat{A}_{mn} - \frac{i}{\hbar}\sum_k\left(\hat{A}_{kn}\mathbf{d}_{km} - \hat{A}_{mk}\mathbf{d}_{nk}\right)\cdot\hat{\mathbf{E}}(\mathbf{r}_A)\,. \tag{10}$$

Formal integration of Eq. (10) yields

$$\hat{A}_{mn}(t) = e^{i\omega_{mn}t}\hat{A}_{mn} - \frac{i}{\hbar}\sum_k \int_0^t dt'\, e^{i\omega_{mn}(t-t')} \times \left[\hat{A}_{kn}(t')\mathbf{d}_{km} - \hat{A}_{mk}(t')\mathbf{d}_{nk}\right]\cdot\hat{\mathbf{E}}(\mathbf{r}_A,t'), \tag{11}$$

which, inserted back into the equation of motion for the dynamical variables of the medium-assisted field, Eq. (9), yields the first iteration of the equations of motion for the dynamical variables as

$$\begin{aligned}\dot{\hat{\mathbf{f}}}(\mathbf{r},\omega,t) &= -i\omega\hat{\mathbf{f}}(\mathbf{r},\omega) + \frac{\omega^2}{c^2}\sqrt{\frac{\operatorname{Im}\varepsilon(\mathbf{r},\omega)}{\hbar\pi\varepsilon_0}}\sum_{m,n} e^{i\omega_{mn}t}\hat{A}_{mn}\mathbf{d}_{mn}\cdot\boldsymbol{G}^*(\mathbf{r}_A,\mathbf{r},\omega)\\ &+\frac{1}{\hbar\pi\varepsilon_0}\sum_{k,m,n}\int_0^t dt'\int_0^\infty d\omega'\int d^3r'\,\frac{\omega^2\omega'^2}{c^4}\sqrt{\operatorname{Im}\varepsilon(\mathbf{r},\omega)\operatorname{Im}\varepsilon(\mathbf{r}',\omega')}e^{i\omega_{mn}(t-t')}\mathbf{d}_{mn}\cdot\boldsymbol{G}^*(\mathbf{r}_A,\mathbf{r},\omega)\\ &\times\left[\hat{A}_{kn}(t')\mathbf{d}_{km} - \hat{A}_{mk}(t')\mathbf{d}_{nk}\right]\cdot\left[\boldsymbol{G}(\mathbf{r}_A,\mathbf{r}',\omega')\cdot\hat{\mathbf{f}}(\mathbf{r}',\omega',t') - \boldsymbol{G}^*(\mathbf{r}_A,\mathbf{r}',\omega')\cdot\hat{\mathbf{f}}^\dagger(\mathbf{r}',\omega',t')\right].\end{aligned} \tag{12}$$

Equation (12) is now a nonlinear operator equation that is capable of describing resonant processes involving two polaritons. This is despite the fact that the original Hamiltonian (1) is bilinear in all operators. The effective nonlinearity appears as a consequence of the iteration. In order to pick out the resonant interactions from the equation of motion, we introduce as usual slowly varying amplitude operators as $\hat{\hat{\mathbf{f}}}(\mathbf{r},\omega,t) = \hat{\mathbf{f}}(\mathbf{r},\omega,t)e^{i\omega t}$ and $\hat{\hat{A}}_{mn}(t) = \hat{A}_{mn}(t)e^{-i\omega_{mn}t}$ and apply the Markov approximation. This involves taking the slowly varying amplitude operators out of the integral at the upper time t.

For our investigation one needs to keep in mind that the polariton spectrum is not continuous but consists of a quasidiscrete set of lines of midfrequencies Ω_k and widths γ_k, where the linewidths are typically very much smaller than the line center separations $\gamma_k \ll (\Omega_{k+1}-\Omega_{k-1})/2$. We then divide the ω axis into intervals $\Delta_k = [(\Omega_{k-1}+\Omega_k)/2, (\Omega_k+\Omega_{k+1})/2]$. Recalling the resonance condition $\Omega_1 \approx \omega_{10}+\Omega_2$, we apply the rotating-wave approximation and finally arrive at the effective equation of motion describing the dynamics of the resonant atom-polariton coupling where now the frequency integrals have to be taken over the linewidth of the surface polaritons,

$$\dot{\hat{\mathbf{f}}}(\mathbf{r},\omega) = -i\omega\hat{\mathbf{f}}(\mathbf{r},\omega) -i\int d^3r'\int_{\Delta_{\omega'}} d\omega'\left[\hat{\mathbf{g}}(\mathbf{r},\mathbf{r}',\omega,\omega')\cdot\hat{\mathbf{f}}(\mathbf{r}',\omega')\right]. \tag{13}$$

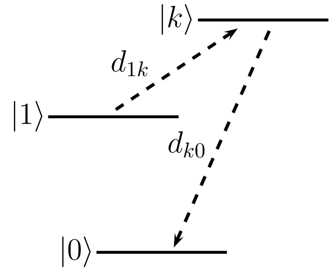

FIG. 2: The transition from $|1\rangle$ to $|0\rangle$ is mediated by the virtual transitions via the state $|k\rangle$.

Here we have introduced the abbreviation

$$\begin{aligned}&\hat{\mathbf{g}}(\mathbf{r},\mathbf{r}',\omega,\omega') =\\ &-\frac{\hat{A}_{10}}{\hbar}\sum_k\left[\frac{\mathbf{d}_{k0}\cdot\boldsymbol{G}_e^*(\mathbf{r}_A,\mathbf{r},\omega)\otimes\mathbf{d}_{1k}\cdot\boldsymbol{G}_e(\mathbf{r}_A,\mathbf{r}',\omega')}{\omega_{k1}+\omega'}\right.\\ &\left.-\frac{\mathbf{d}_{1k}\cdot\boldsymbol{G}_e^*(\mathbf{r}_A,\mathbf{r},\omega)\otimes\mathbf{d}_{k0}\cdot\boldsymbol{G}_e(\mathbf{r}_A,\mathbf{r}',\omega')}{\omega_{0k}+\omega'}\right]\end{aligned} \tag{14}$$

for the operator-valued coupling tensor. As one can see from the structure of $\hat{\mathbf{g}}(\mathbf{r},\mathbf{r}',\omega,\omega')$, the atom-polariton coupling is mediated by a virtual atomic transition from $|1\rangle \to |0\rangle$ via an intermediate state $|k\rangle$ (see Fig. 2) with dipole moments $\mathbf{d}_{1k}$ and $\mathbf{d}_{0k}$. The equation of motion (12) can be thought of as being generated by the effective nonlinear interaction Hamiltonian

$$\hat{H}_{\text{eff}} = \hbar\int d^3r'\int d^3r\int_{\Delta_\omega} d\omega\int_{\Delta_{\omega'}} d\omega'\; \hat{\mathbf{f}}^\dagger(\mathbf{r},\omega)\cdot\hat{\mathbf{g}}(\mathbf{r},\mathbf{r}',\omega,\omega')\cdot\hat{\mathbf{f}}(\mathbf{r}',\omega') - (\omega\leftrightarrow\omega',\ \mathbf{r}\leftrightarrow\mathbf{r}')^*. \tag{15}$$

where the second term describes the process that is obtained by interchanging ω with ω', and $\mathbf{r}$ with $\mathbf{r}'$.

A. Coupling for singly excited polaritons

The interaction energy (15) depends, by virtue of its dependence on the Green function, on the atom-surface distance z and thus contributes to the total Casimir–Polder potential. In the following, we focus on the effective potential that results resulting from this atom-surface coupling. For this purpose, it is useful to define single-polariton excitations (similar to the construction in Ref. [14]) as

$$|1(\mathbf{r}_A,\Omega_i)\rangle = \sqrt{\frac{2}{\pi\gamma_i}} \int\limits_{\Delta_{\Omega_i}} d\omega \int d^3s \, \frac{1}{g(\mathbf{r}_A,\Omega_i)} \times \boldsymbol{G}_e^*(\mathbf{r}_A,\mathbf{s},\omega)\cdot\hat{\mathbf{f}}^\dagger(\mathbf{s},\omega)\,|\{0\}\rangle \tag{16}$$

with the normalization factor

$$g(\mathbf{r}_A,\Omega_i) = \sqrt{\frac{\mu_0}{\hbar\pi}\Omega_i^2 \mathrm{Tr}\,\mathrm{Im}\,\boldsymbol{G}(\mathbf{r}_A,\mathbf{r}_A,\Omega_i)}\,. \tag{17}$$

Using the integral relation (8) for the Green tensor, ine easily checks that the states (16) are indeed properly normalized.

Note that the states $|1(\mathbf{r}_A,\Omega_i)\rangle$ carry a vector index as well as the continuous space and frequency labels. In this approach we assume that the local density of states $\omega^2\mathrm{Im}\,\boldsymbol{G}(\mathbf{r},\mathbf{r},\omega)$ can be approximated by a single Lorentzian peak of mid-frequency Ω and width γ,

$$\omega^2\mathrm{Im}\,\boldsymbol{G}(\mathbf{r},\mathbf{r},\omega) \simeq \Omega^2\mathrm{Im}\,\boldsymbol{G}(\mathbf{r},\mathbf{r},\Omega)\frac{\gamma^2/4}{(\omega-\Omega)^2+\gamma^2/4}\,. \tag{18}$$

In our envisaged situation of a resonant coupling between a single atomic transition and the difference between two polariton resonances, the energies of the initial and final states are identical. Degenerate first-order perturbation theory asserts that the interacting potential is [15]

$$U_{\mathrm{eff}} = \sqrt{\left|\langle K|\,\hat{H}_{\mathrm{eff}}\,|I\rangle\right|^2}. \tag{19}$$

Here $|I\rangle = |1_A\rangle\,|0_1\rangle\,|1_2\rangle$ stands for the tensor product of the initial excited atomic state $|1_A\rangle$ and a singly excited polariton with frequency Ω_2, and $|K\rangle = |0_A\rangle\,|1_1\rangle\,|0_2\rangle$ denotes the tensor product of the final atomic state $|0_A\rangle$ and a single excitation in the polariton with frequency Ω_1. The single-polariton states $|1_\nu\rangle \equiv |1(\mathbf{r}_A,\Omega_\nu)\rangle$ are defined according to Eq. (16) and $|0_\nu\rangle$ denotes the polariton ground state $|0_\nu\rangle = |\{0\}\rangle$, $\forall\omega\in[\Omega_\nu-\delta\omega/2,\Omega_\nu+\delta\omega/2]$.

Using the commutation rules of the operators as well as the properties of the Green functions, together with the definition of the Lorentzian lineshape, Eq. (18), we find that the effective interaction potential can be written in the form

$$\begin{aligned} U_{\mathrm{eff}} = {} & -\frac{\mu_0\Omega_1\Omega_2}{2} \\ & \times\sqrt{\frac{\gamma_1\gamma_2}{\mathrm{Tr}\,\mathrm{Im}\boldsymbol{G}(\mathbf{r}_A,\mathbf{r}_A,\Omega_1)\mathrm{Tr}\,\mathrm{Im}\boldsymbol{G}(\mathbf{r}_A,\mathbf{r}_A,\Omega_2)}} \\ & \sum_k \Bigg\{\mathrm{Tr}\left[\mathrm{Im}\boldsymbol{G}(\mathbf{r}_A,\mathbf{r}_A,\Omega_1)\cdot\mathbf{d}_{0k}\otimes\mathbf{d}_{k1}\cdot\mathrm{Im}\boldsymbol{G}(\mathbf{r}_A,\mathbf{r}_A,\Omega_2)\right] \\ & \times\frac{\Omega_1+\omega_{0k}}{(\Omega_1+\omega_{0k})^2+\gamma_1^2/4} \\ & -\mathrm{Tr}\left[\mathrm{Im}\boldsymbol{G}(\mathbf{r}_A,\mathbf{r}_A,\Omega_1)\cdot\mathbf{d}_{k1}\otimes\mathbf{d}_{0k}\cdot\mathrm{Im}\boldsymbol{G}(\mathbf{r}_A,\mathbf{r}_A,\Omega_2)\right] \\ & \times\frac{\Omega_1+\omega_{k1}}{(\Omega_1+\omega_{k1})^2+\gamma_1^2/4}\Bigg\}. \end{aligned} \tag{20}$$

Comparing Eq. (20) with the Casimir–Polder potential at finite temperature [2, 8],

$$\begin{aligned} \Delta E^{\mathrm{NR}} = {} & \mu_0 k_B T {\sum_{j=0}^{\infty}}' \xi_j^2 \mathrm{Tr}\left[\alpha(i\xi_j)\cdot\boldsymbol{G}(\mathbf{r}_A,\mathbf{r}_A,i\xi_j)\right] \\ & +\mu_0\sum_{k\neq n}\omega_{kn}^2\bar{n}_{\mathrm{th}}(\omega_{kn})\mathbf{d}_{nk}\cdot\mathrm{Re}\,\boldsymbol{G}(\mathbf{r}_A,\mathbf{r}_A,\omega_{kn})\cdot\mathbf{d}_{kn}, \end{aligned} \tag{21}$$

where ξ_j are the Matsubara frequencies, one observes that the effective potential dependence on the atom-surface distance z is given by the same (inverse cubic) power-law as the nonresonant Casimir–Polder potential. This is because the second-order nonlinear Hamiltonian (15) enters only a (degenerate) first-order perturbation theory (19), whereas the nonresonant potential arises from a bilinear Hamiltonian in second-order perturbation theory [2].

The total potential experienced by the atom is the sum of the nonresonant (attractive) CP potential and the resonant coupling between the atoms and the surface polaritons,

$$\Delta E^{\mathrm{Total}} = \Delta E^{\mathrm{NR}} + \Delta E^{\mathrm{R}}. \tag{22}$$

The respective energy shifts for the nonresonant and (second-order) resonant interactions in the nonretarded limit are

$$\begin{aligned} \Delta E^{\mathrm{NR}} = {} & -\frac{\mu_0 c^2 k_B T}{12\pi\hbar z^3}\sum_k|\mathbf{d}_{nk}|^2{\sum_{j=0}^{\infty}}'\frac{\omega_{kn}}{\omega_{kn}^2+\xi_j^2}\frac{\varepsilon(i\xi_j)-1}{\varepsilon(i\xi_j)+1} \\ & +\frac{\mu_0 c^2}{24\pi z^3}\sum_k\bar{n}_{\mathrm{th}}(\omega_{kn})\,|\mathbf{d}_{nk}|^2\,\mathrm{Re}\left[\frac{\varepsilon(\omega_{kn})-1}{\varepsilon(\omega_{kn})+1}\right] \end{aligned} \tag{23}$$

and

$$\Delta E^{\mathrm{R}} = -\frac{\mu_0 \Omega_1 \Omega_2}{2z^3}\sqrt{\frac{\gamma_1\gamma_2}{\mathrm{Tr}\,\mathrm{Im}\boldsymbol{G}'(\Omega_1)\mathrm{Tr}\,\mathrm{Im}\boldsymbol{G}'(\Omega_2)}}$$

$$\times\sum_k \left\{ \mathrm{Tr}\left[\mathrm{Im}\boldsymbol{G}'(\Omega_1)\cdot\mathbf{d}_{0k}\otimes\mathbf{d}_{k1}\cdot\mathrm{Im}\boldsymbol{G}'(\Omega_2)\right] \right.$$

$$\times\frac{\Omega_1+\omega_{0k}}{(\Omega_1+\omega_{0k})^2+\gamma_1^2/4}$$

$$-\mathrm{Tr}\left[\mathrm{Im}\boldsymbol{G}'(\Omega_1)\cdot\mathbf{d}_{k1}\otimes\mathbf{d}_{0k}\cdot\mathrm{Im}\boldsymbol{G}'(\Omega_2)\right]$$

$$\left.\times\frac{\Omega_1+\omega_{k1}}{(\Omega_1+\omega_{k1})^2+\gamma_1^2/4}\right\}, \qquad (24)$$

where we have defined

$$\boldsymbol{G}'(\Omega) = \frac{c^2}{32\pi\Omega^2}\left[\frac{\varepsilon(\Omega)-1}{\varepsilon(\Omega)+1}\right]\begin{pmatrix}1&0&0\\0&1&0\\0&0&2\end{pmatrix} \qquad (25)$$

as the nonretarded scattering Green tensor of a planar halfspace in the coincidence limit $\mathbf{r}\to\mathbf{r}'$, $\boldsymbol{G}'(\Omega)\equiv z^3\boldsymbol{G}(\mathbf{r},\mathbf{r},\Omega)$.

B. Thermal States

As we are dealing with thermally excited surface polaritons the concept of perturbation theory has to be expanded from pure states described by a single state vector to a statistical mixture or ensemble of states [16]. The density matrix for a thermal state with temperature T can be written in the Fock basis $|n\rangle$ as

$$\hat{\rho}_{\mathrm{th}} = \sum_n p_n\,|n\rangle\,\langle n| = \sum_n \frac{e^{-n\hbar\Omega_n/k_BT}}{Z(T)}\,|n\rangle\,\langle n| \qquad (26)$$

where $Z(T) = \sum_m e^{-m\hbar\Omega_m/k_BT}$ denotes the partition function.

So far we have computed the interaction energy for the situation in which there is initially only one excited polariton with frequency Ω_2 and in the final state only one polariton with frequency Ω_1 [see Eq. (19)]. This has to be generalized to thermal states in which there can be initially m polaritons with frequency Ω_1 and n polaritons with frequency Ω_2. In this case, we rewrite the result of the perturbation theory as

$$\left|\langle K|\,\hat{H}_{\mathrm{eff}}\,|I\rangle\right|^2 = \mathrm{Tr}\left[\hat{H}_{\mathrm{eff}}\hat{\rho}_{\mathrm{in}}\hat{H}_{\mathrm{eff}}\,|K\rangle\,\langle K|\right] \qquad (27)$$

where

$$\hat{\rho}_{\mathrm{in}} = \hat{\rho}_{\mathrm{th}}(\Omega_1)\otimes\hat{\rho}_{\mathrm{th}}(\Omega_2)\otimes|1_A\rangle\,\langle 1_A|\,,$$
$$= \sum_{n,m} p_m^{(1)}p_n^{(2)}\,|m_1,n_2\rangle\,\langle m_1,n_2|\otimes|1_A\rangle\,\langle 1_A|\,. \qquad (28)$$

Due to the form of the effective interaction Hamiltonian $\hat{H}_{\mathrm{eff}}$ the only final state $|K\rangle$ that provides a non-vanishing matrix element will be $|K\rangle = |(m+1)_1,(n-1)_2\rangle\,|0_A\rangle$. Hence,

$$\begin{aligned}\left|\langle K|\,\hat{H}_{\mathrm{eff}}\,|I\rangle\right|^2 &= \sum_{m,n} p_m^{(1)}p_n^{(2)}(m+1)_{(1)}(n)_{(2)}U_{\mathrm{eff}}^2,\\ &= \left[\bar{n}_{\mathrm{th}}(\Omega_1)+1\right]\bar{n}_{\mathrm{th}}(\Omega_2)U_{\mathrm{eff}}^2. \qquad (29)\end{aligned}$$

Finally, the resonant energy shift ΔE^R for thermal states will be given as

$$\Delta E^{\mathrm{R}} = U_{\mathrm{eff}}\sqrt{\left[\bar{n}_{\mathrm{th}}(\Omega_1)+1\right]\bar{n}_{\mathrm{th}}(\Omega_2)}. \qquad (30)$$

This result is intuitively clear, as the initial polariton with frequency Ω_2 has to be thermally populated before the resonant interaction can take place.

IV. FINAL REMARKS

The key idea in current experiments is to confine thermal vapours of — typically alkali — atoms in spectroscopy microcells whose thickness lies in the $20-1000$ nm range. These vapour cells are typically made of (transparent) dielectric materials such as sapphire, quartz or fluoride crystals. The nonretarded nonlinear interaction potential between an atom and a dielectric surface is governed by the (nonnegative) dissipative part $\mathrm{Im}\,r_p(\omega)$ of the surface response function, where $r_p(\omega) = (\varepsilon(\omega)-1)/(\varepsilon(\omega)+1)$ is the Fresnel reflection coefficient for p-polarized waves at a planar interface between a dielectric with permittivity $\varepsilon(\omega)$ and free space [see Eq. (25)]. For each dielectric material there is a unique surface polariton spectrum that depends sensitively on the concentration and distribution of the impurities and surface quality of the samples (surface roughness). As each sample is unique, the polariton spectrum should be found experimentally. The Fresnel coefficient $r_p(\omega)$ exhibits resonances (strictly speaking, there are poles in the complex frequency plane where $\varepsilon(\omega) = -1$), the associated modes are the surface polaritons that are linked to the bulk resonances of the dielectric permittivity $\varepsilon(\omega)$.

We use a multi–resonance Drude–Lorentz model

$$\varepsilon(\omega) = 1 + \sum_j \frac{\omega_{Pj}^2}{\omega_{Tj}^2-\omega^2+i\gamma_j\omega}. \qquad (31)$$

with plasma frequencies ω_{Pj} and transverse resonance frequencies ω_{Tj} as an approximate description of the dielectric permittivity. Selecting two well separated resonances, the effective potential becomes

$$\Delta E^{\mathrm{R}} \sim -\frac{\mu_0 c^2}{128\pi z^3}\frac{\omega_{P1}\omega_{P2}}{\sqrt{\Omega_1\Omega_2}}$$

$$\times\sqrt{\left[\bar{n}_{\mathrm{th}}(\Omega_1)+1\right]\bar{n}_{\mathrm{th}}(\Omega_2)}\sum_k \frac{5\,|\mathbf{d}_{0k}|\,|\mathbf{d}_{k1}|}{12}$$

$$\times\left\{\frac{\Omega_1+\omega_{0k}}{(\Omega_1+\omega_{0k})^2+\gamma_1^2/4} - \frac{\Omega_1+\omega_{k1}}{(\Omega_1+\omega_{k1})^2+\gamma_1^2/4}\right\}. \qquad (32)$$

Closer inspection reveals that the interaction is typically dominated by the nonresonant CP potential, whose maximum value for a one-polariton model is

$$\Delta E^{\mathrm{NR}} \sim -\frac{\mu_0 c^2}{48\pi z^3}\frac{k_B T}{\hbar}\sum_\nu \frac{\omega_P^2\,|\mathbf{d}_{1\nu}|^2}{\Omega\omega_{\nu 1}} + \frac{\mu_0 c^2}{24\pi z^3}\sum_\nu \bar{n}_{\mathrm{th}}(\omega_{\nu 1})\,|\mathbf{d}_{1\nu}|^2 \times \mathrm{Re}\left[\frac{\omega_P^2}{2(\omega_T^2-\omega_{1\nu}^2-i\omega_{1\nu}\gamma)+\omega_P^2}\right]. \quad (33)$$

Note that we have considered an isotropic atom in this approach.

Finally, let us investigate which intermediate atomic transitions might provide the largest nonlinear effect. In order to have an effect that is comparable to then nonretarded Casimir–Polder interaction, there has to be a matching atomic transition between energetically close states — note that the transition $|1\rangle \to |0\rangle$ does not need to be allowed by the selection rules — i.e. the intermediate state $|k\rangle$ has to be close to the initial and final states $|1\rangle$ and $|0\rangle$. The reason for this constraint is the rapidly decreasing magnitude of the dipole transition matrix element between states with increasing energy difference. Therefore, the dominant contribution will come from an intermediate state $|k\rangle$ approximately halfway between initial and final states.

In this case the difference between the resonant and nonresonant terms will come from the last line in Eq. (32). Its maximum value is obtained whenever ω_{0k} or ω_{1k} is one of $\Omega_1 \pm \gamma_1/2$; away from these points the numerical value of this term decreases. As we have assumed throughout our calculations that all atomic transitions are far from any single-polariton resonance, the Lorentzian peaks have to be broad, i.e. γ_1 has to be large. This in turn means that, in order for this nonlinear effect to be comparable to the nonresonant CP potential, a strongly dissipative material is needed. For typical cell materials such as sapphire [17] and quartz [18] the resonant nonlinear shift is too small to be relevant for current experimental investigations (only several kHz for Rydberg atoms). In order to access this nonlinear effect, future work will have to focus on investigating suitable cell materials for specific atoms.

Although cell materials that are used in current experiments have usually been studied in depth, experimental findings present large discrepancies, due to variations in the quality of the sample, the degree of its impurities and the oritentation of the crystal axes [19]. Proper (experimental) characterization of the cell material and its resonances is a crucial step in modeling this process.

We would like to acknowledge fruitful discussions with C.S. Adams, H. Kübler and T. Pfau. SR is supported by the PhD grant SFRH/BD/62377/2009 from FCT, cofinanced by FSE, POPH/QREN and EU. This work partially supported by the UK Engineering and Physical Research Council.

[1] H. B. G. Casimir and D. Polder, Physical Review **73** (1948).

[2] S. Scheel and S. Y. Buhmann, Acta Physica Slovaca **58**, 675 (2008).

[3] C. I. Sukenik, M. G. Boshier, D. Cho, V. Sandoghdar, and E. A. Hinds, Physical Review Letters **70**, 560 (1993).

[4] J. Reichel and V. Vuletić, eds., *Atom Chips* (Wiley-VCH Publication, 2011).

[5] A. Gaëtan, Y. Miroshnychenko, T. Wilk, A. Chotia, M. Viteau, D. Comparat, P. Pillet, A. Browaeys, and P. Grangier, Nature Physics Letters **5**, 115 (2009).

[6] E. Urban, T. A. Johnson, T. Henage, L. Isenhower, D. D. Yavuz, T. G. Walker, and M. Saffman, Nature Physics Letters **5**, 110 (2009).

[7] T. F. Gallagher, Reports in Progress on Physics **51**, 143 (1988).

[8] J. A. Crosse, S. A. Ellingsen, K. Clements, S. Y. Buhmann, and S. Scheel, Physical Review A **82**, 010901(R) (2010).

[9] C. Stehle, H. Bender, C. Zimmermann, D. Kern, M. Fleischer, and S. Slama, Nature Photonics **5**, 494 (2011).

[10] J. P. Shaffer, Nature Photonics **5**, 451 (2011).

[11] H. Failache, S. Saltiel, M. Fichet, D. Bloch, and M. Ducloy, Physical Review Letters **83** (1999).

[12] H. Failache, S. Saltiel, A. Fischer, D. Bloch, and M. Ducloy, Physical Review Letters **88** (2002).

[13] H. Kübler, J. P. Shaffer, T. Baluktsian, R. Löw, and T. Pfau, Nature Photonics **4**, 112 (2010).

[14] S. Y. Buhmann and D.-G. Welsch, Physical Review A **77** (2008).

[15] C. Cohen-Tannoudji, B. Diu, and F. Laloe, *Quantum Mechanics*, vol. 2 (Hardcover, Hermann, 1997).

[16] U. Fano, Reviews of Modern Physics **29** (1957).

[17] G. Yu, N. L. Rowell, and D. J. Lockwood, J. Vac. Sci. Technol. A **22** (2004).

[18] W. G. Spitzer and D. A. Kleinman, Physical Review **121**, 1324 (1961).

[19] M.-P. Gorza, S. Saltiel, H. Failache, and M. Ducloy, The European Physical Journal D **15**, 113 (2001).